Optical Properties of Single-Crystal Cadmium†

R. J. Bartlett,* D. W. Lynch, and R. Rosei
Department of Physics and Institute for Atomic Research, Iowa State University, Ames, Iowa 50010
(Received 3 February 1971)

Measurements were made of the reflectivity and/or absorptivity of cadmium from 0.15 to 20 eV, using polarized light with the electric vector both perpendicular and parallel to the c axis of the crystal. In the visible and infrared spectra both polarizations yielded strong absorption peaks. For perpendicular polarization, the main peak was at 0.98 eV and was attributed mainly to transitions between bands along the L-H symmetry line. Also in this polarization there was an absorption edge at 0.29 eV. This may be due to transitions near the point K in the Brillouin zone. For parallel polarization, the main absorption peak was at 1.10 eV and was attributed to transitions between bands along Γ-K, Γ-M, and L-H. No low-energy absorption edge was found for parallel polarization. Agreement between the experimental data and the calculations of Kasowski based on a nonlocal-pseudopotential model was fairly good. There was no agreement between the data and calculations based on a local-pseudopotential model. At low temperatures, the long-wavelength absorptivities were approximately constant, in agreement with theory for the anomalous-skin-effect region. Using the theory of Kliewer and Fuchs and the experimental data, parallel and perpendicular effective masses were calculated to be 1.09 m_0 and 1.61 m_0, respectively. The weighted average of these is in good agreement with the thermal effective mass for cadmium. The low-energy data support the theory of Kliewer and Fuchs and tend to confirm the volume absorption process suggested by Holstein.

INTRODUCTION

We have measured the reflectivity R and/or absorptivity $A = 1 - R$ of single crystals of cadmium at several temperatures and over a wide range of photon energies. From these measurements the two components of the dielectric tensor ($\tilde{\epsilon} = \epsilon_1 + i\epsilon_2$), i.e., with the electric field parallel and perpendicular to the c axis, have been found by Kramers-Kronig analysis. Interband absorption extends from about 0.3 to above 9 eV, with the main structure being confined to the 0.3–2.5-eV region.

The interband absorption can be computed from energy band calculations. It was first thought that a local-pseudopotential calculation would give good band structures for polyvalent metals.[1,2] If so, then the interband absorption should consist of sharp peaks in $\omega\epsilon_2$ at energies of twice the important pseudopotential Fourier coefficients, with a high-energy tail on each peak.[2–5] At least two local-pseudopotential calculations have been made for cadmium,[2,6] but they do not have the same pseudopotential Fourier coefficients. Even though the coefficients of Ref. 6 were adjusted to give a Fermi surface in agreement with some experimental data, they do not agree at all with our results. Stark and Falicov[7] showed that a nonlocal-pseudopotential calculation is necessary and carried out such a calculation for Zn and Cd. The conduction bands originate from the two 5s levels of the Cd atom, but they must be orthogonalized to the 4d levels of the cores. The 4d levels do not overlap the conduction band, but lie just below it, giving a large k-dependent contribution to the pseudopotential. The bands of Stark and Falicov agreed well with available Fermi surface data. Kasowski[8] then used these bands to calculate the components of ϵ_2 parallel and perpendicular to the c axis for both Zn and Cd. His calculations were made at two temperatures, and predicted an easily observed temperature effect due to changes in the pseudopotential which are caused by lattice vibrations and the anisotropic thermal expansion. His results for Zn are in many respects in fairly good agreement with recent measurements by Rubloff.[9] The calculated ϵ_2 for Cd has the same shape as our results, but too large a magnitude. (The calculated ϵ_2 is in even worse agreement with earlier data on Cd.[10]) Comparison of optical data with calculations based on bands known to fit Fermi-surface data enables one to test the bands several eV above and below the Fermi level.

In addition to interband effects, our infrared data at 4 K allow us to determine, subject to several assumptions, the electron-effective-mass components. Our data in this region are in agreement with current models for the anomalous skin effect and absorption mechanisms at low temperature.

EXPERIMENTAL METHODS

Samples were spark cut from a single crystal of Cominco 99.9999% cadmium. They were polished with emery, then with Al_2O_3, followed by four or

five applications of an etch and distilled water rinses. The etch was 66.7 g of CrO_3 and 5 g of Na_2SO_4 in 333 ml of H_2O. After the final etch, the samples were washed in distilled water for 5 min and hot methanol for several minutes, dried in nitrogen, and placed directly in a sample chamber which was then evacuated. Samples cut with a c axis in the face were used to obtain both components of $\tilde{\epsilon}$. As a check, a sample with the c axis normal to the face gave the $\perp$ component of $\tilde{\epsilon}$ when used at near-normal incidence.

Data were taken by three methods.

(i) In the infrared and visible at 4 K, a calorimetric technique was used to obtain A between 0.15 and 3 eV. This method has been described elsewhere,[11–13] except that a polarizer was used (AgCl pile-of-plates or a Glan prism). The relative errors in A ranged from 2% at 1 eV to 5 or 10% at 0.15 eV.

(ii) From 0.6 to 6 eV the reflectivity was measured in a Cary 14R spectrophotometer using Glan prism polarizers and a reflectometer similar to that of Hartman and Logothetis.[14] Even at 300 K the samples were in an evacuated cryostat to retard oxidation. Data were taken at 300, 78, and 12 K. The accuracy of R is estimated to be about 3%.

(iii) From 4 to 20 eV, data were taken using polarized uv light produced by synchrotron radiation from electrons.[15–17] The source was the 240-MeV electron storage ring operated by the Physical Sciences Laboratory of the University of Wisconsin. The light was dispersed by a 1-m normal-incidence monochromator with a 1200-line/mm grating blazed for 1200 Å. The light was chopped by a tuning fork and detected by a sodium salicylate-coated 1P28 photomultiplier. The photomultiplier was on an arm which rotated in the sample chamber to receive reflected light from the sample. The sample could be rotated in order to vary the angle of incidence. Thus the reflectivity could be measured at a variety of angles of incidence. (The sample could be removed from the beam so the detector could receive the incident light.) The incident intensity varied with time because of loss of electrons in the storage ring, but this loss was monitored (and corrected for) by a sodium salicylate-coated beam splitter and another photomultiplier. Both photomultiplier signals were synchronously detected and recorded.

Part of the reflectometer rotated so that s- or p-polarized light was incident on the sample. Measurements of the polarization of the beam were made using a polarizer made of four gold mirrors at a 60° angle of incidence.[18,19] The degree of polarization always exceeded 70%. A filter of LiF revealed a large amount of long-wavelength scattered light (50% at 12.5 eV) in the beam reflected from the sample. Because the reflectivity of Cd is high at long wavelengths and small at short ones, this scattered light necessitated a very large correction, which was made. However, because the correction was so large, we report only the normal incidence reflectivity data, and use it chiefly to show that there seems to be no structure at high energy and to give us data for Kramers-Kronig analysis of our low-energy results.

In all cases, we used non-normal incidence (although often it was as near normal as possible). If the plane of incidence in a reflection measurement is normal to the c axis, then the two measured reflectivities are

$$R_s = \left| \frac{(\tilde{\epsilon}_{\parallel} - \sin^2\phi)^{1/2} - \cos\phi}{(\tilde{\epsilon}_{\parallel} - \sin^2\phi)^{1/2} + \cos\phi} \right|^2 \tag{1}$$

and

$$R_p = \left| \frac{\tilde{\epsilon}_{\perp}\cos\phi - (\tilde{\epsilon}_{\perp} - \sin^2\phi)^{1/2}}{\tilde{\epsilon}_{\perp}\cos\phi + (\tilde{\epsilon}_{\perp} - \sin^2\phi)^{1/2}} \right|^2 , \tag{2}$$

where ϕ is the angle of incidence. For small ϕ we can set $\sin^2\phi = \phi^2$, $\cos^2\phi = 1 - (\phi^2/2)$, and, using $\tilde{\epsilon} = (n + ik)^2$, we find

$$R_s(\phi) = R_s(0)(1 + 2\phi^2 n_{\parallel}/n_{\parallel}^2 + k_{\parallel}^2) \tag{3}$$

and

$$R_p(\phi) = R_p(0)(1 - 2\phi^2 n_{\perp}/n_{\perp}^2 + k_{\perp}^2) . \tag{4}$$

We assumed $\phi = 0$ for our near-normal incidence data, computed $\tilde{\epsilon}$ by Kramers-Kronig analysis, then used the resultant $\tilde{\epsilon}$ in (3) and (4) to convert our $R(\phi)$ to $R(0)$. Further iteration in (3) and (4) makes less than a 0.1% change. It is $R(0)$ which we further analyze.

RESULTS

Figures 1 and 2 show the absorptivities of Cd at 4.2 K. The very weak structure for $\vec{E} \perp \hat{c}$, a shoulder at 0.29 eV, was confirmed by using a sample with the c axis normal to its face and unpolarized light for higher sensitivity. This structure is reminiscent of a weak structure recently found in the "free-carrier region" of Al.[20] (We have also detected a similar structure at 0.4 eV in Zn, again only for $\vec{E} \perp \hat{c}$, but it is a bit harder to see.) The peak at 0.98 eV for $E \perp \hat{c}$ is very sharp and high. It is followed by a broad peak between 1.4 and 1.8 eV. For $\vec{E} \parallel \hat{c}$ there is a sharp peak at 1.10 eV with no peak or shoulder at higher energy, but with a very small reproducible peak at its onset, 0.8 eV. Figure 3 shows the room-temperature reflectivity from 0.6 to 5.6 eV. (The 0–0.6-eV line represents a free-electron gas extrapolation.) The sharp peak seen in each polarization is considerably broadened, and the broad peak for $\vec{E} \perp \hat{c}$ is not observed. Figure 4 shows the high-energy reflectivity, which has been normalized to match that of Fig. 3 between 5 and 6 eV.

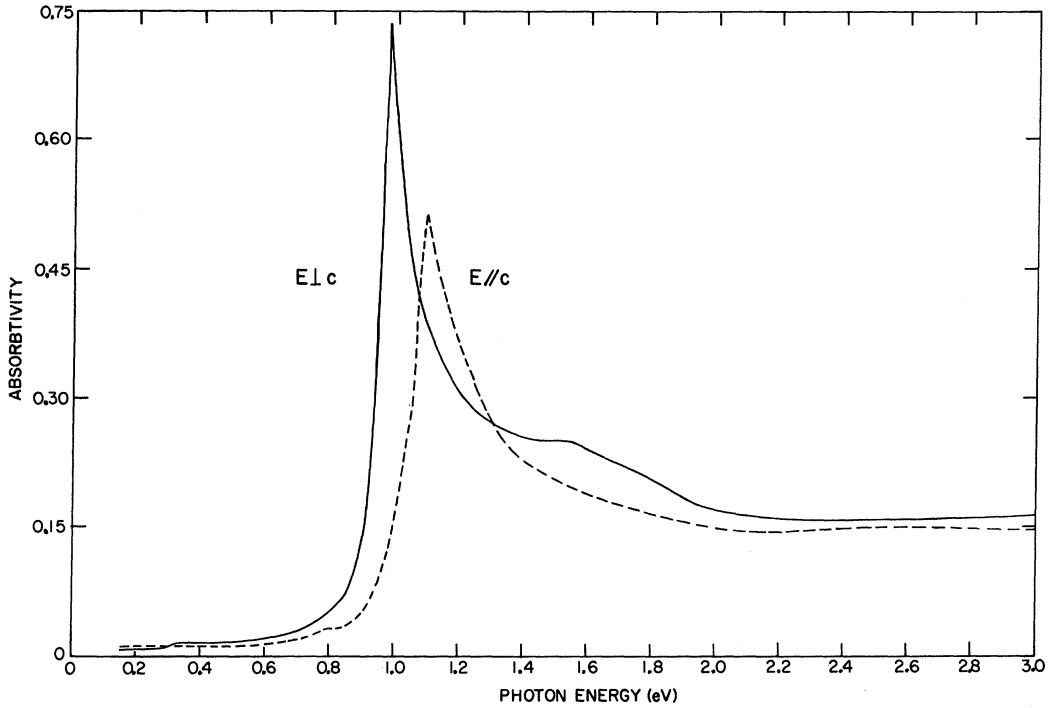

FIG. 1. Absorptivity of Cd at 4.2 K. The spectral band pass near 1 eV is 0.025 eV, 15° angle of incidence.

Our results agree with those of others on opaque films[21] and single crystals, [22] except that in Ref. 21, a gradual rise in reflectivity occurs above 10 eV, and the drop in reflectivity between 4 and 6 eV is more gradual than ours.

The data may be influenced by a layer of CdO

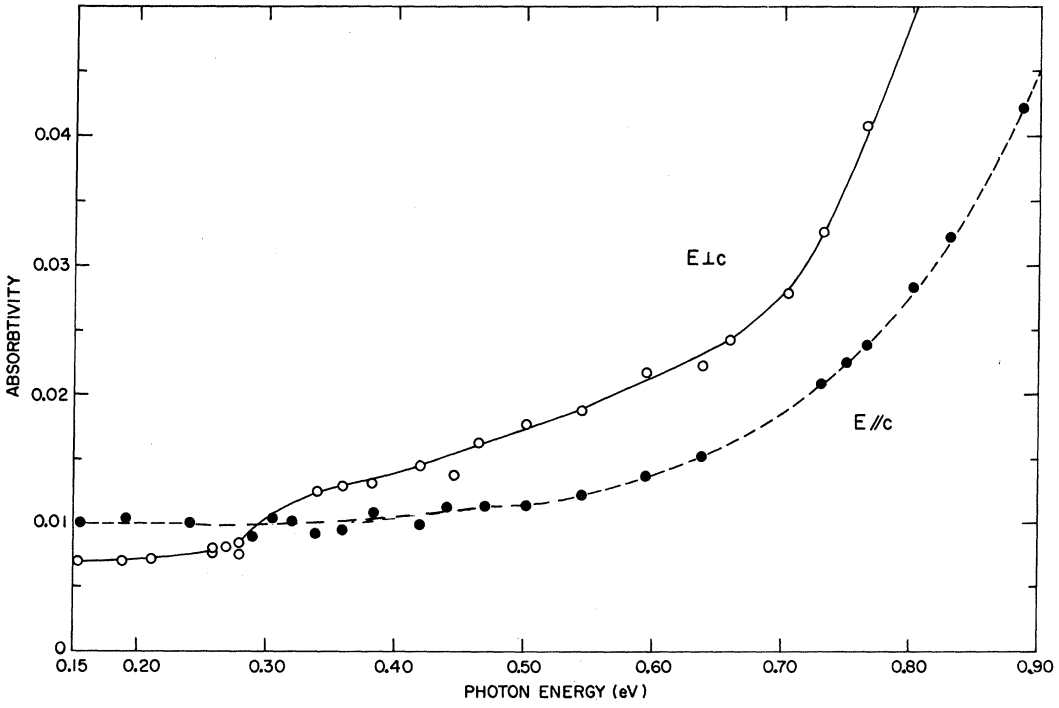

FIG. 2. Absorptivity of Cd at 4.2 K—low-photon-energy region.

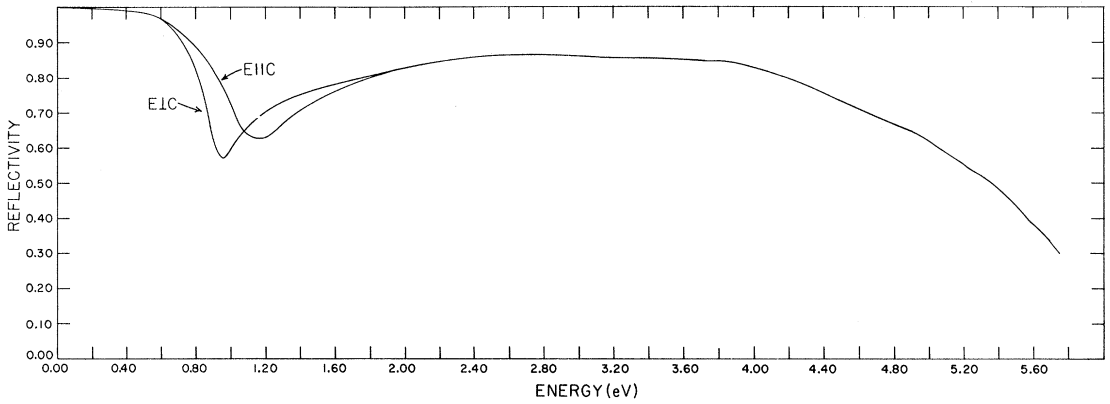

FIG. 3. Reflectivity of Cd at 300 K and 15° angle of incidence.

on the surface. CdO begins to absorb at about 2 eV, and shows a strong absorption peak at 10 eV.[23] We have three checks on the effects of oxidation: (a) Using a well-collimated monochromatic light beam, reflectivity measurements were made with *s* polarization at angles of incidence of 15°, 30°, 45°, 60°, and 75° on a Cd crystal with the *c* axis normal to the basal plane.[24] Using our data for $\tilde{\epsilon}_\perp$ (see below), we calculated the reflectivity to be expected at each angle. Agreement was excellent (1%) for all angles at 2 eV, but became progressively worse at 3, 4, and 5 eV, especially at larger angles where the path length through any absorbing CdO becomes larger. This indicates the probable presence of some oxide, but its effect below 2 eV should be small, negligible for our purposes. (b) The reflectivity drops off rapidly between 4 and 6 eV. Mosteller and Wooten[25] show that when a vacuum-cleaved Zn crystal is oxidized, the corresponding sharp drop in reflectivity turns into a more gradual drop. Thus we expect our samples to have oxidized less rapidly than similarly treated Zn samples. (c) By using the spectrum of $\tilde{\epsilon}$ for CdO,[23] we can calculate a cor-

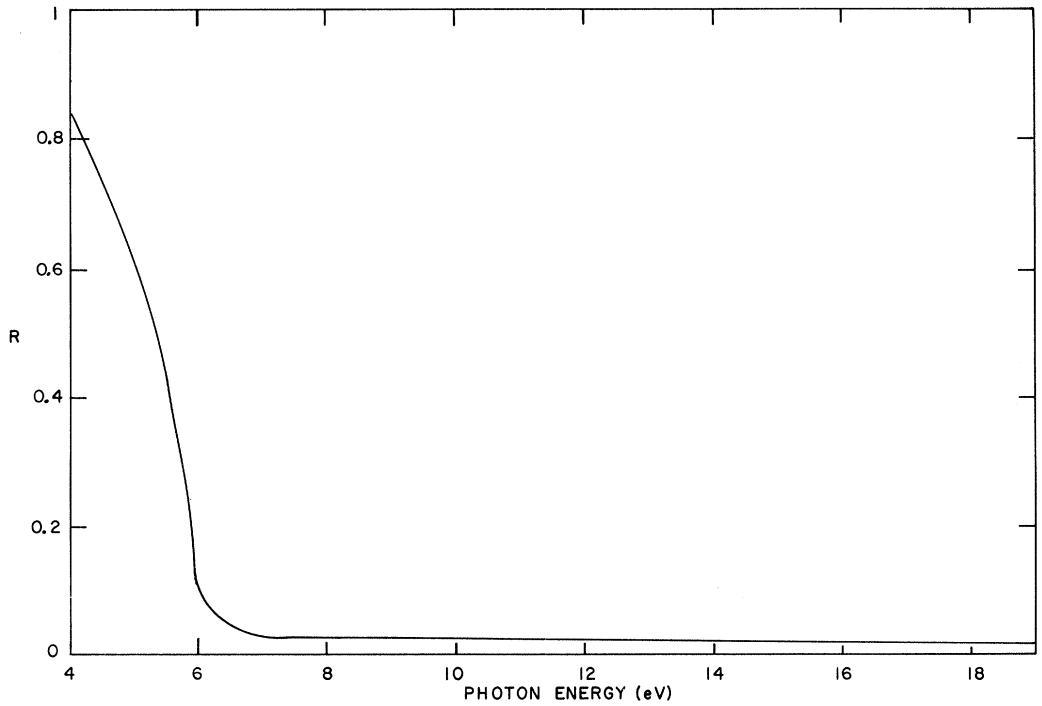

FIG. 4. Reflectivity of Cd at 300 K— high-photon-energy region, 15° angle of incidence, $\vec{E} \perp \hat{c}$.

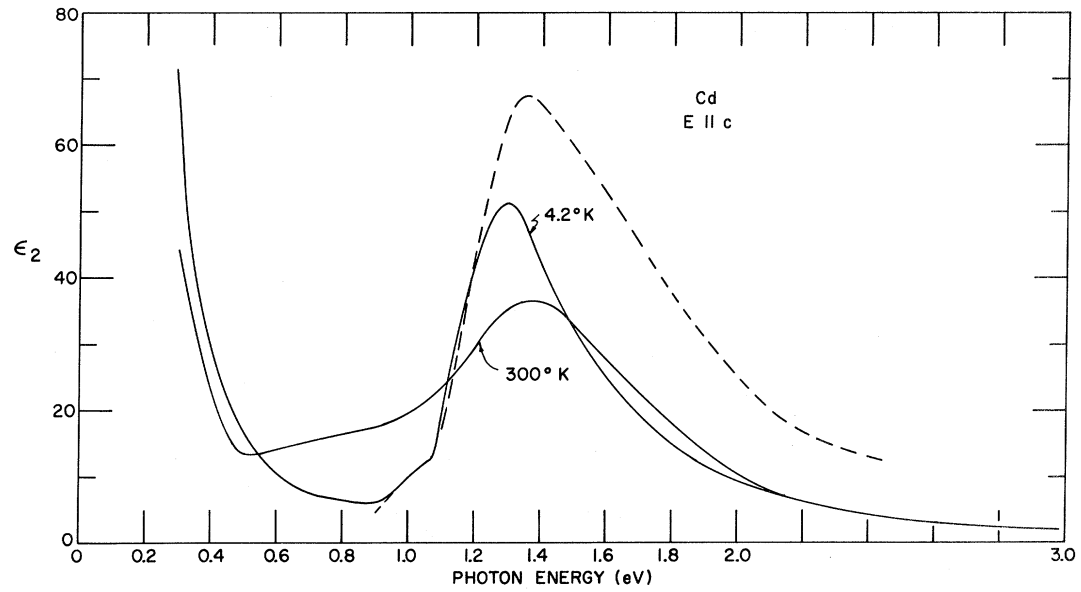

FIG. 5. Imaginary part of the dielectric constant of Cd for $\vec{E} \parallel \hat{c}$. The dashed curve is from the 4.2-K data but corrected for an assumed layer of CdO on the surface 35 Å thick.

rection for the presence of CdO on our samples by assuming various thicknesses of oxide. This was done, and thicknesses up to 35 Å could occur. If larger thicknesses were assumed, negative values of ϵ_2 for the Cd resulted. The effect of the oxide was to make the true ϵ_2 curves for Cd higher near the main peak than those originally obtained, but the general appearance of the ϵ_2 spectra was not altered (Figs. 5 and 6). For our purposes this is what is important. Moreover, in the discussion of Figs. 9 and 10, we can show that a 35-Å layer of CdO is probably too thick. The effect of CdO on the infrared absorptivity is not small (as it is on the infrared reflectivity), and it is subsumed in a parameter in the analysis.

The data were then analyzed by using a Kramers-

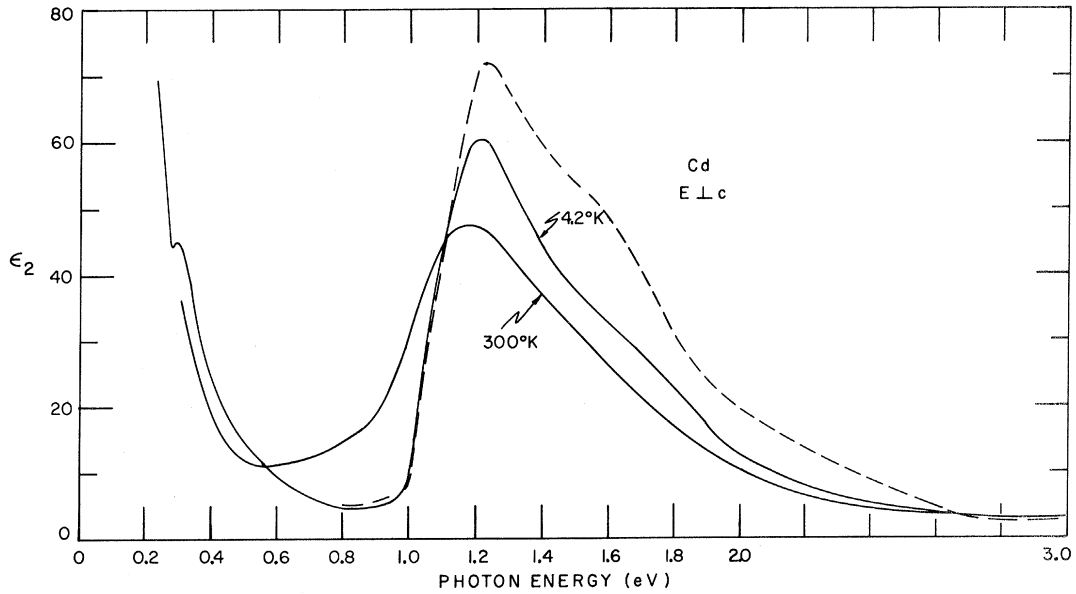

FIG. 6. Imaginary part of the dielectric constant of Cd for $\vec{E} \perp \hat{c}$. The dashed curve is from the 4.2-K data but corrected for an assumed layer of CdO on the surface 35 Å thick.

Kronig integral on R to get the phase α of the amplitude reflection coefficient. From R and α,

$$n = \frac{1-R}{1+R-2\sqrt{R}\cos\alpha} \quad , \tag{5}$$

$$k = \frac{2R\sin\alpha}{1+R-2\sqrt{R}\cos\alpha} \quad , \tag{6}$$

$$\epsilon_1 = n^2 - k^2 \quad , \tag{7}$$

$$\epsilon_2 = 2nk \quad . \tag{8}$$

From 20 to 100 eV we assumed that R fell linearly to 0.01%. Other extrapolations did not affect the shape of the ϵ_2 spectra at all, and had less than a 10% effect on the height of the peak in ϵ_2. In the infrared, a Drude extrapolation was used at 300 K, and a constant R at 4 K.

Figure 5 shows ϵ_2 for $\vec{E}\parallel\hat{c}$ at 300, 4.2, and 4.2 K as corrected for an assumed layer of CdO 35 Å thick. Figure 6 shows the same for $\vec{E}\perp\hat{c}$. Figures 7 and 8 show ϵ_2/λ for $\vec{E}\parallel\hat{c}$ and $\vec{E}\perp c$, respectively, including previous data[10] and the calculated data of Kasowski.[8] Our data are qualitatively in agreement with those of Graves and Lenham,[10] taken on mechanically polished surfaces, but are higher.

As a further check on the absolute magnitude of our ϵ_2 curves, we can calculate the partial sum rule for ϵ_2:

$$N_{\text{eff}}(E) = \frac{4}{\pi(\hbar\omega_p)}\, 2\int_0^E E\epsilon_2(E)\,dE \quad , \tag{9}$$

where $\hbar\omega_p$ is the conduction-electron plasmon energy and $N_{\text{eff}}(E)$ is the number of electrons per atom contributing to optical absorption at energies below E. For an isotropic free-electron gas of two electrons/atom in Cd, $\hbar\omega_p = 11.3$ eV. Equation (9)

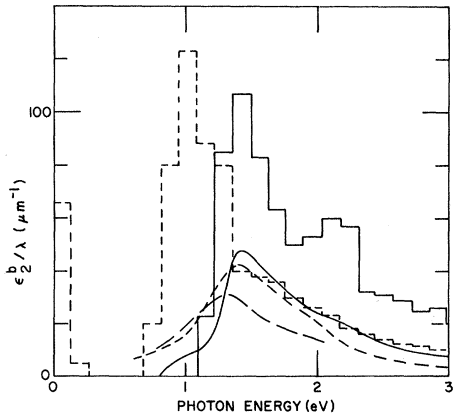

FIG. 7. ϵ_2/λ for Cd, $\vec{E}\parallel\hat{c}$. Solid curve, our data, 4 K; solid histogram, calculated values (Ref. 8), 4 K; dashed curve, our data, 300 K; dashed histogram, calculated values (Ref. 8), 462 K; lowest dashed curve, data of Ref. 10, 300 K.

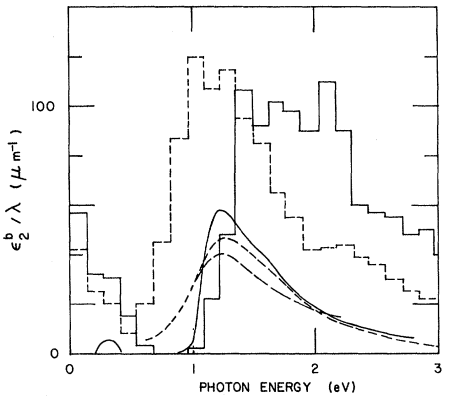

FIG. 8. ϵ_2/λ for Cd, $\vec{E}\perp\hat{c}$. Solid curve, our data, 4 K; solid histogram, calculated values (Ref. 8), 4 K; dashed curve, our data, 300 K; dashed histogram, calculated values (Ref. 8), 462 K; lowest dashed curve, data of of Ref. 10, 300 K.

has a factor of 4 before the integral, twice the usual factor. This is the result of using two electrons/atom in $\hbar\omega_p$. N_{eff} then saturates at two electrons/atom when ϵ_2 for a free-electron gas is used in Eq. (9). The results of putting our data into Eq. (9) are shown in Figs. 9 and 10. A discussion of the low-energy contribution to (9) is given in an Appendix. For $\vec{E}\parallel\hat{c}$ (Fig. 9), the correction to the 4-K curve for 35 Å of CdO clearly makes N_{eff} too high. The addition of any Drude term at 0.15 eV will raise the curves by $N_{\text{eff}}^D(0.15\text{ eV})$, making $N_{\text{eff}}(3\text{ eV})$ well above two electrons/atom. Since transitions from the $4d$ levels are not expected[22] for energies below 9 eV, N_{eff} should not exceed two electrons/atom. Thus, once again we see that CdO layers, if present, are below 35 Å in thickness. The rise in N_{eff} at high energies is believed to be an artifact of the Kramers-Kronig analysis.

DISCUSSION

Interband Region

If the electron energy bands in Cd can be calculated from a local pseudopotential, the structure in ϵ_2/λ should consist of peaks at energies corresponding to twice the important Fourier coefficients of the pseudopotential. Thus for $\vec{E}\parallel\hat{c}$, there should be peaks at $2|V_{000,2}|$ and $2|V_{110,1}|$, while for $\vec{E}\perp\hat{c}$, the peaks should be at $2|V_{110,1}|$ and $2|V_{110,0}|$. These peaks might be shifted by broadening effects. Our data would then give $2|V_{000,2}| = 1.05$ eV, $2|V_{1\bar{1}0,0}| = 0.29$ eV, and $2|V_{110,1}| = 1.10$ eV, qualitatively different from other values.[2,6] Moreover, the areas under the peaks should be proportional to $n_g g\cos^2\theta_g f|V_g|$, where the Fourier coefficient V_g splits n_g equivalent planes in $\vec{k}$ space,

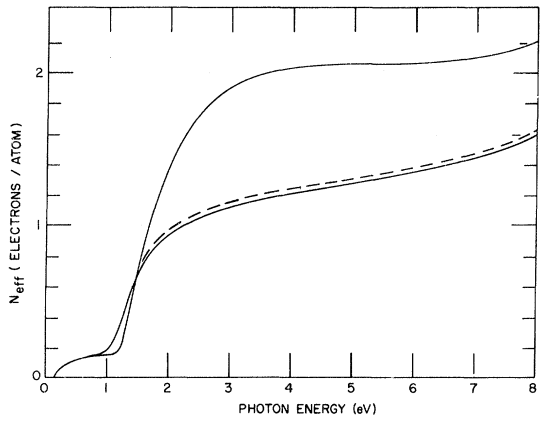

FIG. 9. Effective number of electrons contributing to absorption below energy E. Cadmium, $\vec{E} \parallel \hat{c}$. Solid line, 4 K; dashed line, 300 K; upper line, 4-K data with correction for 35-Å layer of CdO.

and θ_g is the angle between the electric field and $\vec{g}$, a reciprocal-lattice vector.[5] For $\vec{g} = (110, 0)$, this predicts the 1.10-eV peak will have relative areas of 2.3:1 for $\vec{E} \perp$ and $\parallel$ to $\hat{c}$. This is clearly not observed, even though some of the spectrum for $\vec{E} \parallel c$ should come from $2|V_{000,2}|$.

Before comparing our data with the calculations of Kasowski,[8] it is necessary to subtract the free-carrier contribution to ϵ_2. This was done simply by subtracting the free-carrier part of ϵ_2 and its high-energy extrapolation in Figs. 5 and 6 from the total ϵ_2 in these figures. This should introduce no errors that would qualitatively alter our conclusions. Figure 7 shows such a corrected ϵ_2/λ for $\vec{E} \parallel \hat{c}$ at 4 K, along with the calculated values. The position and width of the main peak agree with the calculated values, but the calculated height is about a factor of 2 too large, both in the peak and in the high-energy tail. For $\vec{E} \perp \hat{c}$ (Fig. 8), the width is again about right but the calculated peak is located about 0.25 eV too high. The calculated result is really a double peak,[8] and the experimental high-energy portion of this doublet is probably the weak shoulder near 1.6 eV. Again, the calculated ϵ_2 values are too large, especially for the second peak. The low-energy peak near 0.3 eV is also much smaller than the calculated result, but the calculations become very "noisy" at such low energies. The general agreement of the peak positions and shapes indicates that the calculated band structures are probably correct in the large. The fact that the calculated ϵ_2 values are generally too large is probably the result of too large electric dipole matrix elements, which are notoriously difficult to calculate accurately.

The single peak for $\vec{E} \parallel \hat{c}$ is the result of two types of transitions—a double peak due to transitions near L (which also occur for $\vec{E} \perp \hat{c}$) and transitions along Γ-H and Γ-K. For $\vec{E} \perp \hat{c}$, there are only the transitions near L. (The low-energy peak at 0.3 eV may arise from transitions near K.) According to the calculation, which neglects the effect of thermal broadening in ϵ_2, raising the temperature weakens the pseudopotential coefficients, causing a shift of the bands. The result of this is a merging of the double hump to give a single peak for both polarizations, a peak which is *higher* and *narrower* at 462 K than at 0 K. It is also shifted to lower energy, and some low energy (< 0.6 eV) interband absorption is predicted to occur for both polarizations. We see a red shift upon warming, and the broad peak near 1.6 eV has merged with the sharp peak at 0.98 eV. If the total width of both peaks is considered, there is a slight decrease in the width of the peak upon warming. However, the height of the peak decreases with increasing temperature, contrary to the predicted behavior.

Free-Electron Region

Our high-energy data cannot be used to find the plasmon frequency. The sharp drop in reflectivity at 6 eV (Fig. 4) looks like a plasma edge, but interband transitions from the 4*d* band may affect the reflectivity spectrum. Experimental values of $\hbar\omega_p$ range from 7.5 to 9.1 eV,[26] all below the free-electron value of 11.3 eV. Our curves of ϵ_1 are nearly parallel to the energy axis, so a small error in ϵ_1 results in a large error in the zero of ϵ_1, an estimate of the plasmon energy. Similar large errors arise in the position of the peak of the calculated electron energy loss function, $-\mathrm{Im}(\tilde{\epsilon}^{-1})$, the plasmon energy. (One must also note that CdO has a peak in ϵ_2 near 8 eV,[23] which may influence any measurements near the plasma resonance.) We thus can study only the infrared.

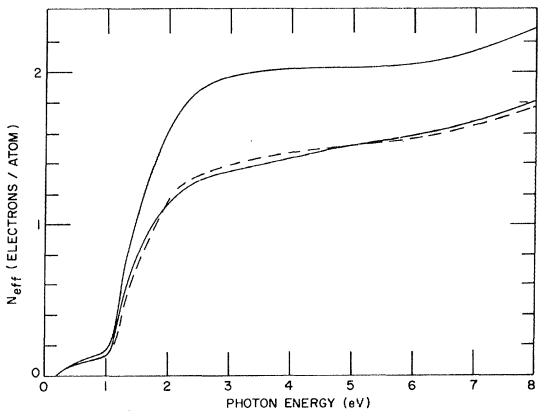

FIG. 10. Effective number of electrons contributing to absorption below energy E. Cadmium, $\vec{E} \perp \hat{c}$. Solid line, 4 K; dashed line, 300 K; upper line, 4-K data with correction for 35-Å layer of CdO.

To this end, we made measurements of the resistivity ratios of spark-cut samples of our Cd crystal. The results were

$$(\rho_{300}/\rho_{4.2})_{\parallel} = 15.0\times10^{3}$$

and

$$(\rho_{300}/\rho_{4.2})_{\perp} = 11.6\times10^{3} \ .$$

In addition the resistivity anisotropy was measured at two temperatures,

$$(\rho_{\perp}/\rho_{\parallel})_{300} = 0.90$$

and

$$(\rho_{\perp}/\rho_{\parallel})_{4.2} = 1.17 \ .$$

(The literature value[27] of the resistivity anisotropy at 293 K is 0.82 instead of 0.90. The discrepancy may be the result of geometrical errors in our results. These errors do not affect the "reversal" of the anisotropy upon going to 4 K.)

Our infrared intraband data exist only at 4 K, where the Drude model, or any local model, is inadequate. Here the mean free path is not small compared with the penetration depth of the light, and a local relation between electric field and current density does not exist.[28] Reuter and Sondheimer[29] presented a theory for this, the anomalous skin effect, for both specular and diffuse reflection of electrons at the surface. The theory has subsequently been expanded to treat non-normal incidence.[30–33]

As the crystal is cooled, the relaxation time τ lengthens, and the Drude model predicts A should fall; but instead, A drops a bit upon cooling and then stays constant. A conduction electron can absorb a photon only if the electron scatters, allowing energy and momentum to be conserved. Reuter and Sondheimer considered scattering at the surface, since bulk scattering processes were unlikely, and derived for diffuse scattering the expression $A = \frac{3}{4}v/c$, where v is the Fermi velocity. Later Holstein[34,35] showed that there were bulk processes within the penetration depth giving rise to an additional absorption so that

$$A = \tfrac{3}{4}v/c + 2\gamma' + 2\gamma'' \ . \qquad (10)$$

γ' here is a measure of the scattering, and is $\gamma' = (\omega_p\tau)^{-1}$, where ω_p is the free-electron plasma frequency and τ the relaxation time. Normally at low temperatures we find that $2\gamma' \ll \frac{3}{4}(v/c)$. $\gamma'' = (\omega_p\tau'')^{-1}$, where τ'' is an effective relaxation time for the new process Holstein envisioned, the absorption of a photon and emission of a phonon. It is given approximately by

$$\tau'' = \tfrac{5}{2}(T\tau/\Theta) \ , \qquad (11)$$

where Θ is the Debye temperature and τ is the actual relaxation time, determined by the dc resistivity, at temperature $T > \Theta$. This additional volume term has been sought experimentally and tentatively identified.[11,12,36,37] It has been seen clearly in recent far-infrared work[38] on Pb, but the description is not as simple[39] as Eq. (11) when the photon and phonon energies are comparable. Fuchs and Kliewer[33] have generalized Eq. (10) including, among other corrections, non-normal incidence. For s polarization, they find

$$A = 2\gamma\cos\phi[1 - \tfrac{1}{8}(\gamma/\Omega)^2 + \tfrac{1}{2}\Omega^2\cos^2\phi - \gamma\cos\phi]$$
$$+ \tfrac{3}{4}(v/c)\cos\phi[1 - (\gamma/\Omega)^2 - 2\gamma\cos\phi]$$
$$- (v/c)^2\cos\phi[\tfrac{65}{128}(\gamma/\Omega^2) + \tfrac{9}{32}\cos\phi] \ , \qquad (12)$$

where ϕ is the angle of incidence and $\Omega = \omega/\omega_p$, a dimensionless frequency. In Eq. (12), γ would be $(\gamma' + \gamma'')$ of Eq. (10).

As Fig. 2 shows, at 4 K, A becomes constant at long wavelengths. For $\vec{E}\parallel\hat{c}$, $A = 0.010$. For $\vec{E}\perp\hat{c}$, $A = 0.007$. To evaluate v/c we are forced to use free-electron values—there is no information available on the anisotropy of v/c. This gives $\frac{3}{4}v/c = 0.004$. γ' is negligible for our high-resistivity ratio samples. The observed anisotropy in A will then come from γ''. Using literature values of dc conductivity[27] ($\sigma_{\parallel} = 1.30\times10^{7}\ \Omega^{-1}\,\mathrm{m}^{-1}$, $\sigma_{\perp} = 1.58\times10^{7}\ \Omega^{-1}\,\mathrm{m}^{-1}$), Debye temperature[40] (209 K), and the (isotropic) free-electron plasma frequency, we calculate via Eq. (11) $A_{\parallel} = 0.0103$ from Eq. (12), in good agreement with the experimental value of 0.010. The anisotropy in A is then assumed to reside in γ'' and to enter as the anisotropy in τ''. Equation (10) yields $A_{\parallel} = 0.0125$. This is poorer agreement with the measured value, but it is still reasonable agreement in view of the assumptions in the calculation of τ''. (The assumption about the isotropy of v is not important because $\frac{3}{4}v/c$ is so small.) To get $A_{\perp}$ we used p-polarized light and $\phi = 15°$; but Eq. (12) is not valid for finite ϕ and p polarization. [Equation (10) is also valid only at $\phi = 0$.] If we set $\phi = 0$, Eq. (10) gives $A_{\perp} = 0.0099$ and Eq. (12) gives $A_{\perp} = 0.0094$, both in rather poor agreement with the measured 0.007. We can not pinpoint the source of the discrepancy.

If we use Eq. (12), we can force agreement with experiment by adjusting the effective masses. This is done by finding an effective mass m^* and relaxation time τ that yield the dc room-temperature conductivity and the low-temperature infrared absorptivity via Eqs. (11) and (12). The results are

$$m_{\parallel}^* = 1.09m_0$$

and

$$m_{\perp}^* = 1.61m_0 \ ,$$

where m_0 is the electron rest mass. From these an optic (isotropic) effective mass can be calculated as

$$m^*_{opt} = \tfrac{1}{3}(2m^*_{\perp} + m^*_{\parallel}) \ . \tag{13}$$

This gives $m^*_{opt} = 1.44m$, in very good agreement with the thermal effective mass obtained from the linear term in the low-temperature specific heat measurements,[41] $m^*_t = 1.45m_0$. This agreement is expected only if the electron-phonon enhancement of the thermal effective mass[42] is small, otherwise we expect $m^*_t > m^*_{opt}$. Recent calculations[43] indicate that the phonon mass enhancement of m^*_t should not exceed about 12% for Zn and Cd, and at 4 K it should be smaller than this.

ACKNOWLEDGMENTS

We wish to acknowledge the assistance of C. G. Olson in making the large-angle reflectivity measurements and of those responsible for running the electron storage ring, especially C. H. Pruett, E. M. Rowe, and R. Otte.

APPENDIX

Our data begin at 0.15 eV at 4 K and 0.6 eV at 300 K. It is difficult to evaluate reliably N_{eff} [Eq. (9)] for E below these values. A Drude expression for ϵ_2

$$\epsilon_2^D = \frac{\omega_p^2 \tau}{\omega(1+\omega^2\tau^2)}$$

leads to

$$N^D_{eff}(E) = (4/\pi)\tan^{-1}(\tau E/\hbar) \ ,$$

where τ is the electron relaxation time obtained from the dc conductivity. Interband transitions, beginning at E_0, cause $N^D_{eff}(E)$ to decrease for $E < E_0$ because of the f-sum rule. This can be taken into account by using an effective mass in ϵ_2^D for $E < E_0$, but with τ determined from the dc conductivity, this leads to N^D_{eff} (0.15 eV) ~ 1 electron/atom. N^D_{eff} is very sensitive to τ, and it is not clear that the dc value is appropriate—literature values of τ determined from infrared data often are smaller than the dc values by factors of 2 or 3, lowering N^D_{eff} by similar factors. Our measurements cannot be used to get reliable values of τ.

We have used smooth extrapolations of the reflectivity at 300 K to perform the Kramers-Kronig analysis. This gives us curves of ϵ_2 between 0 and 0.6 eV which are not Drude-like—τ must depend on E or ϵ_2 must be given by a sum of Drude-like terms with different parameters. These ϵ_2 spectra give N_{eff}(0.15 eV) of about 0.24 electrons/atom and N^D_{eff}(0.6 eV) of about 0.3 electrons/atom, which seem reasonable.

In Figs. 9 and 10 we have refrained from estimating N^D_{eff} at the energy where our data begin. The curves for 4 K start at $N_{eff} = 0$ at 0.15 eV. The curves for 300 K were moved vertically to match the 4-K curves at 1 eV.

---

†Work performed at the Ames Laboratory of the U.S. Atomic Energy Commission, Contribution No. 2928. Storage ring supported by U.S. Air Force Office of Scientific Research.

*Present address: School of Physics, Georgia Institute of Technology, Atlanta, Ga. 30332.

[1]W. A. Harrison, *Pseudopotentials in the Theory of Metals* (Benjamin, New York, 1966).

[2]W. A. Harrison, Phys. Rev. 147, 467 (1966).

[3]R. N. Gurzhi and G. P. Motulevich, Zh. Eksperim. i Teor. Fiz. 51, 1220 (1966) [Sov. Phys. JETP 24, 818 (1967)].

[4]A. I. Golovashkin, I. S. Levchenko, G. P. Motulevich, and A. A. Shubin, Zh. Eksperim. i Teor. Fiz. 51, 1622 (1966) [Sov. Phys. JETP 24, 1093 (1967)].

[5]A. I. Golovashkin, A. I. Kopeliovich, and G. P. Motulevich, Zh. Eksperim. i Teor. Fiz. 53, 2053 (1967) [Sov. Phys. JETP 26, 1161 (1968)].

[6]S. Katsuki and M. Tsuji, J. Phys. Soc. Japan 20, 1136 (1965).

[7]R. W. Stark and L. M. Falicov, Phys. Rev. Letters 19, 795 (1967).

[8]R. V. Kasowski, Phys. Rev. 187, 885 (1969).

[9]G. W. Rubloff, Phys. Rev. B 3, 285 (1971).

[10]R. H. W. Graves and A. P. Lenham, J. Opt. Soc. Am. 58, 126 (1968).

[11]M. A. Biondi and J. A. Rayne, Phys. Rev. 115, 1522 (1959).

[12]M. A. Biondi and A. I. Guobadia, Phys. Rev. 166, 667 (1968).

[13]L. W. Bos and D. W. Lynch, Phys. Rev. B 2, 4567 (1970).

[14]P. L. Hartman and E. Logothetis, Appl. Opt. 3, 255 (1964).

[15]K. Codling and R. P. Madden, J. Appl. Phys. 36, 380 (1965).

[16]R. Haensel and C. Kunz, Z. Angew. Phys. 23, 276 (1967).

[17]R. P. Godwin, Springer Tracts Mod. Phys. 50, 1 (1969).

[18]R. N. Hamm, R. A. McRae, and E. T. Arakawa, J. Opt. Soc. Am. 55, 1460 (1965).

[19]G. Rosenbaum, B. Feuerbacher, R. P. Godwin, and M. Skibowski, Appl. Opt. 7, 1917 (1968).

[20]L. W. Bos and D. W. Lynch, Phys. Rev. Letters 25, 156 (1970).

[21]W. C. Walker, O. P. Rustgi, and G. C. Weissler, J. Opt. Soc. Am. 49, 471 (1959).

[22]S. Robin-Kandare, J. Robin, S. Kandare, and S. Jerič, Compt. Rend. 257, 1605 (1963); 257, 2026 (1963).

[23]M. Altwein, H. Finkenrath, Č. Koňák, J. Stuke, and G. Zimmerer, Phys. Status Solidi 29, 203 (1968).

[24]R. J. Bartlett and C. G. Olson (unpublished).

[25]L. P. Mosteller and F. Wooten, Phys. Rev. 171, 743 (1968).

[26]B. Feuerbacher and B. Fitton, Phys. Rev. Letters 24, 499 (1970), and references therein.
[27]G. T. Meaden, *Electrical Resistance of Metals* (Plenum, New York, 1965).
[28]A. B. Pippard, Proc. Roy. Soc. (London) A191, 385 (1947).
[29]G. E. H. Reuter and E. H. Sondheimer, Proc. Roy. Soc. (London) A195, 336 (1948).
[30]F. Forstmann, Z. Physik 203, 495 (1967).
[31]K. L. Kliewer and R. Fuchs, Phys. Rev. 172, 607 (1968).
[32]R. Fuchs and K. L. Kliewer, Phys. Rev. 185, 905 (1969).
[33]K. L. Kliewer and R. Fuchs, Phys. Rev. B 2, 2923 (1970).
[34]T. Holstein, Phys. Rev. 88, 1427 (1952).
[35]T. Holstein, Phys. Rev. 96, 535 (1954).
[36]M. A. Biondi, Phys. Rev. 102, 964 (1956).
[37]J. A. Rayne, Phys. Rev. Letters 3, 512 (1956).
[38]R. R. Joyce and P. L. Richards, Phys. Rev. Letters 24, 1007 (1970).
[39]H. Scher, Phys. Rev. Letters 25, 759 (1970).
[40]N. E. Phillips, Phys. Rev. 134, A385 (1965).
[41]D. L. Martin, Proc. Phys. Soc. (London) 78, 1482 (1961).
[42]N. W. Ashcroft and J. W. Wilkins, Phys. Letters 14, 285 (1965).
[43]P. B. Allen and M. L. Cohen, Phys. Rev. B 1, 1329 (1970).

PHYSICAL REVIEW B VOLUME 3, NUMBER 12 15 JUNE 1971

Magnetic Surface Levels in a Tipped Magnetic Field*

S. P. Singhal†

and

R. E. Prange
Department of Physics and Astronomy and Center for Theoretical Physics, University of Maryland, College Park, Maryland 20742
(Received 23 December 1970)

The wave functions and spectrum for metallic electrons skipping along a surface in a magnetic field are calculated for general orientation of field and surface relative to the crystal axes of the material. Unlike the case in which the field is parallel to the surface, the energy levels form a continuum rather than a discrete set of bound magnetic surface levels. Nevertheless, except for rather extreme tip angles, no broadening or change of shape of the observed signals should be observed. In general there will be a rescaling of the field variable which can be used to measure Fermi-surface quantities inaccessible by other techniques. The analysis of the data is somewhat more complex than in the parallel-field case, however.

I. INTRODUCTION

The experimental study of magnetic surface levels[1–5] has proved to be extraordinarily useful in determining a wide variety of parameters characterizing a metallic system. These include Fermi-surface parameters (velocities, radii of curvature, and masses[6] as a function of temperature[7]), lifetimes (also as a function to temperature),[8] and properties of the metal-vacuum interface.[9] The latter includes static and dynamic roughness (Rayleigh waves)[10] and the probability of specular reflection as a function of glancing angle.[11,12]

One reason for the great interest in these measurements is that the observed properties, in a given experiment, are associated with a given point on the Fermi surface (or more accurately, with a given small region of the Fermi surface). Thus, for example, one is able to measure lifetimes as a function of position on the Fermi surface.[8]

Various modification of these experiments have been proposed,[13] and some of them have been carried out.[14,15] These have led to new results.

The purpose of this paper is to analyze another modification of the experiment which is easy to carry out experimentally, although it is surprisingly difficult to attack theoretically.

The basic experiment is a measurement of the surface impedance as a function of magnetic field when that field is applied parallel to the surface. The crucial electrons are those at the Fermi surface which are travelling nearly parallel to the real surface (assumed to be the plane $z=0$) and of maximal (or extremal) velocity perpendicular to the magnetic field (say, in the y direction). Thus the important electrons are those of energy E at the Fermi energy E_F, velocity $V_z \sim 0$, and the maximum V_x consistent with the previous conditions.[16]

These electrons are curved into the surface repeatedly by the Lorentz force $F_z = -eV_x B/c$ and skip repeatedly in very shallow hops along the surface (see Fig. 1). Thus their motion is periodic